Mechanism and Machine Theory 45 (2010) 967–980

Contents lists available at ScienceDirect

Mechanism and Machine Theory

journal homepage: www.elsevier.com/locate/mechmt

Effect of the joint inertia on selection of under-actuated control algorithm for flexible-link manipulators

Mohamed W. Mehrez, Ayman A. El-Badawy *

Dept. of Mechatronics Engineering, The German University in Cairo, Cairo, Egypt

ARTICLE INFO

Article history:
Received 18 August 2009
Received in revised form 9 February 2010
Accepted 8 March 2010

Keywords:
Flexible manipulator
Joint inertia
Computed torque
Singular perturbation

ABSTRACT

In this paper, two control techniques, namely computed torque law and composite control based on the singular perturbation approach, are used to control the motion of a flexible-link manipulator. The effect of manipulator joint inertia on the selection of the control technique used has been investigated. It is found that, unlike composite control, the joint inertia increases the oscillations of the flexible arm when the arm is commanded to follow a certain trajectory under the computed torque control law alone. On the other hand, when we exclude the joint inertias, while modeling the flexible arm, there is no significant difference between the system response based on singular perturbation approach and that based on the computed torque method.

1. Introduction

Most existing robotic manipulators are designed to maximize stiffness, in an attempt to minimize system vibration and achieve good positional accuracy. High stiffness is achieved by using heavy material. As a consequence, such robots are usually heavy with respect to the operating payload. This, in turn, limits the speed of operation of the robot manipulation. In contrast, flexible robot manipulators exhibit many advantages over their rigid counterparts: they require less material, are lighter in weight, have higher manipulation speed, are more maneuverable and transportable, are safer to operate, have less overall cost and higher payload to robot weight ratio [1]. However, the problems due to the distributed link flexibility and the resulting vibrations often lead to long settling times and position inaccuracy in lightweight manipulators. Hence, it is essential to develop comprehensive dynamic models for this type of manipulator that consider all these factors. This will enable improved control techniques to be devised so that performance can be optimized [2].

For robots with flexible links, the end-effector trajectory tracking problem is solved in [3] based on the iterative computation of the link deformations associated with the desired output motion, combined with a state trajectory regulator. The problem of active damping of flexural vibrations of the robot links by only the joint control inputs have been addressed in [4], where the authors developed a controller based on end-point sensing and the rigid Jacobian of the manipulator. Experimental investigations into the development of feedforward and feedback control schemes for vibration control of a very flexible and high-friction manipulator system was developed in [1], where a feedforward control scheme based on input shaping and low-pass filtering techniques and a strain feedback control scheme are examined. The performances of the controllers are assessed in terms of the input tracking capability and vibration reduction as compared to the response with PD control. Ider et al. [5] developed a full-state feedback control after linearizing the dynamic equations of a two-link robot with flexible links. In [6], a method for synthesizing the feedforward torques and reference trajectory for a flexible two-link planar manipulator is proposed. The control law for each drive torque consists of two parts: a commanded feedforward torque and a linear angular position and velocity feedback.

* Corresponding author. Tel.: +20 12 744 7745; fax: +20 2 2758 1041.
E-mail address: ayman.elbadawy@guc.edu.eg (A.A. El-Badawy).

0094-114X/$ – see front matter © 2010 Elsevier Ltd. All rights reserved.
doi:10.1016/j.mechmachtheory.2010.03.003

A model of *N*-link flexible manipulators is derived and reformulated in the form of singular perturbation theory [7] and an integral manifold is used to separate fast dynamics from slow dynamics. A composite control algorithm is proposed for the flexible robots, which consists of two main parts. Fast control, u_f, guarantees that the fast dynamics remains asymptotically stable. Slow control, u_s, consists of a robust PD designed based on the rigid model [8]. In [9], the hybrid control scheme is proposed to stabilize the vibration of a two-link flexible manipulator while the robustness of Variable Structure Control (VSC) developed for rigid manipulators is maintained for controlling the joint angels. An experimental study of a robust control scheme for flexible-link robotic manipulators is presented in [10], where the design is based on a simple strategy for trajectory tracking which exploits the two-time scale nature of the flexible part and the rigid part of the dynamic equations of this kind of robotics arms.

The effect of the manipulator joint inertia on the response of the arm is presented in this paper. The joint inertia is usually due to the gear ratio, as most motors utilize gear boxes. This gear ratio increases the joint inertia by a factor that is proportional to the square of that gear ratio. So, it is important to consider the joint inertia while modeling the manipulator. Also, any improvement in the response of the arm without the need for extra actuators, like piezoelectric actuators, would be desirable. A study on a one link flexible arm (with and without joint inertia) is performed in this paper. The step response of the system under both the computed-torque and composite control laws, which both output the same number of control signals, will be compared.

2. Flexible arm dynamic equations

A common way of modeling flexible robot manipulators consists of using a combined Lagrange-assumed modes approach, which allows deriving a dynamic model in closed form. The equations of motion of an n links flexible arm with m_i being the number of modes used to describe the deflection of link i can be written in the form [11,12].

$$\mathbf{M}(\boldsymbol{\theta},\boldsymbol{\delta})\begin{bmatrix}\ddot{\boldsymbol{\theta}}\\ \ddot{\boldsymbol{\delta}}\end{bmatrix}+\begin{bmatrix}\mathbf{f}_1\left(\boldsymbol{\theta},\dot{\boldsymbol{\theta}}\right)\\ \mathbf{f}_2\left(\boldsymbol{\theta},\dot{\boldsymbol{\theta}}\right)\end{bmatrix}+\begin{bmatrix}\mathbf{g}_1\left(\boldsymbol{\theta},\dot{\boldsymbol{\theta}},\boldsymbol{\delta},\dot{\boldsymbol{\delta}}\right)\\ \mathbf{g}_2\left(\boldsymbol{\theta},\dot{\boldsymbol{\theta}},\boldsymbol{\delta},\dot{\boldsymbol{\delta}}\right)\end{bmatrix}+\begin{bmatrix}\mathbf{0}\\ \mathbf{K}\boldsymbol{\delta}\end{bmatrix}=\begin{bmatrix}\mathbf{T}\\ \mathbf{0}\end{bmatrix} \tag{1}$$

where $\mathbf{M}=\begin{bmatrix}\mathbf{M}^{rr} & \mathbf{M}^{re}\\ \mathbf{M}^{er} & \mathbf{M}^{ee}\end{bmatrix}$ is the inertia matrix, superscripts r and e refer to rigid body (joint) and elastic degrees of freedom respectively. $\boldsymbol{\theta}=[\theta_1 \ldots \theta_n]^T$ is the vector of joint variables, $\boldsymbol{\delta}=[\delta_{11} \ldots \delta_{1m1}\ \delta_{21} \ldots \delta_{2mm}]^T$ is the vector of deflection variables, $\mathbf{f_1}$ and $\mathbf{f_2}$ are the vectors containing gravitational (only in $\mathbf{f_1}$), Coriolis, and centrifugal terms, $\mathbf{g_1}$ and $\mathbf{g_2}$ are the vectors which account for the interaction of joint variables and their time derivatives with deflection variable and their time derivatives, $\mathbf{K}$ is a diagonal matrix whose diagonal sub-matrices are the stiffness matrices of links in terms of the deflection variables, $\mathbf{u}=[\mathbf{T}\ \mathbf{0}]^T$, where $\mathbf{T}$ is the vector of joints torques.

3. Flexible arm control

In this section, two control techniques are presented, the computed torque control, and a composite control based on the singular perturbation approach. The computed torque control [13] is a common control technique that is used for rigid manipulators, where the control signal is computed through

$$\mathbf{T}=\mathbf{M}^{rr}\left[\ddot{\boldsymbol{\theta}}_d+\mathbf{k}_v\left(\dot{\boldsymbol{\theta}}_d-\dot{\boldsymbol{\theta}}\right)+\mathbf{k}_p(\boldsymbol{\theta}_d-\boldsymbol{\theta})\right]+\mathbf{f}_1 \tag{2}$$

where in $\mathbf{M}^{rr}$ and $\mathbf{f_1}$, δ*s* are set to zero. $\mathbf{k}_v$ and $\mathbf{k}_p$ are the velocity and position feedback gain diagonal matrices respectively. $\boldsymbol{\theta}_d$, $\dot{\theta}_d$, and $\ddot{\theta}_d$ are the desired trajectory position, velocity, and acceleration respectively. In the following subsections, a composite control based on singular perturbation approach is derived.

3.1. Singularly perturbed model

Consider now the equations of motion given by Eq. (1). Since the inertia Matrix $\mathbf{M}$ is positive definite, then it can be inverted and denoted by $\mathbf{H}$, which can be partitioned as follows:

$$\mathbf{M}^{-1}=\mathbf{H}=\begin{bmatrix}\mathbf{H}_{11[n\times n]} & \mathbf{H}_{12[n\times m]}\\ \mathbf{H}_{21[m\times n]} & \mathbf{H}_{22[m\times m]}\end{bmatrix} \tag{3}$$

Now, Eq. (1) become

$$\ddot{\boldsymbol{\theta}}=-\mathbf{H}_{11}\mathbf{f}_1-\mathbf{H}_{12}\mathbf{f}_2-\mathbf{H}_{11}\mathbf{g}_1-\mathbf{H}_{12}\mathbf{g}_2-\mathbf{H}_{12}\mathbf{K}\boldsymbol{\delta}+\mathbf{H}_{11}\mathbf{T} \tag{4a}$$

$$\ddot{\boldsymbol{\delta}}=-\mathbf{H}_{21}\mathbf{f}_1-\mathbf{H}_{22}\mathbf{f}_2-\mathbf{H}_{21}\mathbf{g}_1-\mathbf{H}_{22}\mathbf{g}_2-\mathbf{H}_{22}\mathbf{K}\boldsymbol{\delta}+\mathbf{H}_{21}\mathbf{T} \tag{4b}$$

The flexible dynamic system Eqs. (4a) and (4b) is characterized by $n+m$ generalized coordinates but only n control inputs. Therefore the synthesis of a nonlinear feedback control is not as easy as for rigid arm (a control input for each joint).

A model order reduction is made by the use of singular perturbation theory leading to a composite control for the full order system [14]. The reduced order system is presented now.

Following [8], a singularly perturbed model of the dynamic system (4) can be obtained as follows. Assume that the orders of magnitude of the **K** matrix elements ($k_i's$) are comparable. It is appropriate to extract a common scale factor k (the smallest spring constant, for instance) such that

$$k_i = k\tilde{k}_i,\ i = 1,\ \ldots,\ m. \tag{5}$$

The following new variables (elastic forces) can be defined:

$$\boldsymbol{\zeta} = k\tilde{\mathbf{k}}\boldsymbol{\delta} \tag{6}$$

$$\tilde{\mathbf{k}} = diag\left(\tilde{k}_1 \cdots \tilde{k}_m\right) \tag{7}$$

The next step is to define $\mu = 1/k$ and obtain

$$\begin{aligned}\ddot{\boldsymbol{\theta}} = &-\mathbf{H}_{11}(\boldsymbol{\theta},\mu\boldsymbol{\zeta})\mathbf{f}_1\left(\boldsymbol{\theta},\dot{\boldsymbol{\theta}}\right)-\mathbf{H}_{12}(\boldsymbol{\theta},\mu\boldsymbol{\zeta})\mathbf{f}_2\left(\boldsymbol{\theta},\dot{\boldsymbol{\theta}}\right)\\ &-\mathbf{H}_{11}(\boldsymbol{\theta},\mu\boldsymbol{\zeta})\mathbf{g}_1\left(\boldsymbol{\theta},\dot{\boldsymbol{\theta}},\mu\boldsymbol{\zeta},\mu\dot{\boldsymbol{\zeta}}\right)-\mathbf{H}_{12}(\boldsymbol{\theta},\mu\boldsymbol{\zeta})\mathbf{g}_2\left(\boldsymbol{\theta},\dot{\boldsymbol{\theta}},\mu\boldsymbol{\zeta},\mu\dot{\boldsymbol{\zeta}}\right)\\ &-\mathbf{H}_{12}(\boldsymbol{\theta},\mu\boldsymbol{\zeta})\boldsymbol{\zeta}+\mathbf{H}_{11}(\boldsymbol{\theta},\mu\boldsymbol{\zeta})\mathbf{T}\end{aligned} \tag{8a}$$

$$\begin{aligned}\mu\ddot{\boldsymbol{\zeta}} = &-\mathbf{H}_{21}(\boldsymbol{\theta},\mu\boldsymbol{\zeta})\mathbf{f}_1\left(\boldsymbol{\theta},\dot{\boldsymbol{\theta}}\right)-\mathbf{H}_{22}(\boldsymbol{\theta},\mu\boldsymbol{\zeta})\mathbf{f}_2\left(\boldsymbol{\theta},\dot{\boldsymbol{\theta}}\right)-\mathbf{H}_{21}(\boldsymbol{\theta},\mu\boldsymbol{\zeta})\mathbf{g}_1\left(\boldsymbol{\theta},\dot{\boldsymbol{\theta}},\mu\boldsymbol{\zeta},\mu\dot{\boldsymbol{\zeta}}\right)\\ &-\mathbf{H}_{22}(\boldsymbol{\theta},\mu\boldsymbol{\zeta})\mathbf{g}_2\left(\boldsymbol{\theta},\dot{\boldsymbol{\theta}},\mu\boldsymbol{\zeta},\mu\dot{\boldsymbol{\zeta}}\right)-\mathbf{H}_{22}(\boldsymbol{\theta},\mu\boldsymbol{\zeta})\boldsymbol{\zeta}+\mathbf{H}_{21}(\boldsymbol{\theta},\mu\boldsymbol{\zeta})\mathbf{T}\end{aligned} \tag{8b}$$

which is a singularly perturbed model of the flexible arm. Notice that all quantities on the right hand side of Eq. (8b) have been conveniently scaled by $\tilde{\mathbf{k}}$.

It can be shown that as $\mu \to 0$, the model of the rigid manipulator is obtained from (8a and 8b). Formally, setting $\mu = 0$ and solving for $\boldsymbol{\zeta}$ in Eq. (8b) one obtains

$$\begin{aligned}\bar{\boldsymbol{\zeta}} = &\mathbf{H}_{22}^{-1}\left(\bar{\boldsymbol{\theta}},0\right)\left[-\mathbf{H}_{21}\left(\bar{\boldsymbol{\theta}},0\right)\mathbf{f}_1\left(\bar{\boldsymbol{\theta}},\dot{\bar{\boldsymbol{\theta}}}\right)-\mathbf{H}_{21}\left(\bar{\boldsymbol{\theta}},0\right)\mathbf{g}_1\left(\bar{\boldsymbol{\theta}},\dot{\bar{\boldsymbol{\theta}}},0,0\right)+\mathbf{H}_{21}\left(\bar{\boldsymbol{\theta}},0\right)\bar{\mathbf{T}}\right]\\ &-\mathbf{f}_2\left(\bar{\boldsymbol{\theta}},\dot{\bar{\boldsymbol{\theta}}}\right)-\mathbf{g}_2\left(\bar{\boldsymbol{\theta}},\dot{\bar{\boldsymbol{\theta}}},0,0\right)\end{aligned} \tag{9}$$

where the over bars are used to indicate that the system with $\mu = 0$ is considered. Plugging Eq. (9) into Eq. (8a) yields

$$\ddot{\bar{\boldsymbol{\theta}}} = \left[\mathbf{H}_{11}\left(\bar{\boldsymbol{\theta}},0\right)-\mathbf{H}_{12}\left(\bar{\boldsymbol{\theta}},0\right)\mathbf{H}_{22}^{-1}\left(\bar{\boldsymbol{\theta}},0\right)\mathbf{H}_{21}\left(\bar{\theta},0\right)\right]\times\left[-\mathbf{f}_1\left(\bar{\theta},\dot{\bar{\boldsymbol{\theta}}}\right)+\bar{\mathbf{T}}\right] \tag{10}$$

where

$$\mathbf{H}_{11}\left(\bar{\boldsymbol{\theta}},0\right)-\mathbf{H}_{12}\left(\bar{\boldsymbol{\theta}},0\right)\mathbf{H}_{22}^{-1}\left(\bar{\boldsymbol{\theta}},0\right)\mathbf{H}_{21}\left(\bar{\boldsymbol{\theta}},0\right) = \mathbf{M}_{11}^{-1}\left(\bar{\boldsymbol{\theta}}\right) \tag{11}$$

where $\mathbf{M}_{11}(\bar{\theta})$ is the $[n\times n]$ positive definite matrix for the rigid-link arm. Hence, $\mathbf{f}_1$ is exactly the function of $\boldsymbol{\theta}$ and $\dot{\theta}$ appearing in the rigid-arm model.

Choosing $\mathbf{x}_1 = \boldsymbol{\theta}$, $\mathbf{x}_2 = \dot{\boldsymbol{\theta}}$, and $\mathbf{z}_1 = \boldsymbol{\zeta}$, $\mathbf{z}_2 = \varepsilon\dot{\boldsymbol{\zeta}}$ with $\varepsilon = \sqrt{\mu}$ gives the state-space form of the system (8a and 8b);i.e.

$$\begin{aligned}\dot{\mathbf{x}}_1 &= \mathbf{x}_2,\\ \dot{\mathbf{x}}_2 &= -\mathbf{H}_{11}\left(\mathbf{x}_1,\varepsilon^2\mathbf{z}_1\right)\mathbf{f}_1(\mathbf{x}_1,\mathbf{x}_2)-\mathbf{H}_{12}\left(\mathbf{x}_1,\varepsilon^2\mathbf{z}_1\right)\mathbf{f}_2(\mathbf{x}_1,\mathbf{x}_2)\\ &\quad-\mathbf{H}_{11}\left(\mathbf{x}_1,\varepsilon^2\mathbf{z}_1\right)\mathbf{g}_1\left(\mathbf{x}_1,\mathbf{x}_2,\varepsilon^2\mathbf{z}_1,\varepsilon\mathbf{z}_2\right)\\ &\quad-\mathbf{H}_{12}\left(\mathbf{x}_1,\varepsilon^2\mathbf{z}_1\right)\mathbf{g}_2\left(\mathbf{x}_1,\mathbf{x}_2,\varepsilon^2\mathbf{z}_1,\varepsilon\mathbf{z}_2\right)\\ &\quad-\mathbf{H}_{12}\left(\mathbf{x}_1,\varepsilon^2\mathbf{z}_1\right)\mathbf{z}_1+\mathbf{H}_{11}\left(\mathbf{x}_1,\varepsilon^2\mathbf{z}_1\right)\mathbf{T}\end{aligned} \tag{12a}$$

$$\begin{aligned}\varepsilon\dot{\mathbf{z}}_1 &= \mathbf{z}_2,\\ \varepsilon\dot{\mathbf{z}}_2 &= -\mathbf{H}_{21}\left(\mathbf{x}_1,\varepsilon^2\mathbf{z}_1\right)\mathbf{f}_1(\mathbf{x}_1,\mathbf{x}_2)-\mathbf{H}_{22}\left(\mathbf{x}_1,\varepsilon^2\mathbf{z}_1\right)\mathbf{f}_2(\mathbf{x}_1,\mathbf{x}_2)\\ &\quad-\mathbf{H}_{21}\left(\mathbf{x}_1,\varepsilon^2\mathbf{z}_1\right)\mathbf{g}_1\left(\mathbf{x}_1,\mathbf{x}_2,\varepsilon^2\mathbf{z}_1,\varepsilon\mathbf{z}_2\right)\\ &\quad-\mathbf{H}_{22}\left(\mathbf{x}_1,\varepsilon^2\mathbf{z}_1\right)\mathbf{g}_2\left(\mathbf{x}_1,\mathbf{x}_2,\varepsilon^2\mathbf{z}_1,\varepsilon\mathbf{z}_2\right)\\ &\quad-\mathbf{H}_{22}\left(\mathbf{x}_1,\varepsilon^2\mathbf{z}_1\right)\mathbf{z}_1+\mathbf{H}_{21}\left(\mathbf{x}_1,\varepsilon^2\mathbf{z}_1\right)\mathbf{T}\end{aligned} \tag{12b}$$

At this point, singular perturbation theory requires that the slow subsystem and the fast (boundary layer) subsystem be identified. The slow subsystem is formally obtained by setting $\varepsilon = 0$, i.e., the rigid model of the arm of the arm obtained above

$$\begin{aligned}\dot{\bar{\mathbf{x}}}_1 &= \bar{\mathbf{x}}_2 \\ \dot{\bar{\mathbf{x}}}_2 &= \mathbf{M}_{11}^{-1}(\bar{\mathbf{x}}_1)\left[-\mathbf{f}_1(\bar{\mathbf{x}}_1, \bar{\mathbf{x}}_2) + \bar{\mathbf{T}}\right]\end{aligned} \tag{13}$$

To derive the fast subsystem, we introduce the fast time scale $\tau = t/\varepsilon$. Then it can be recognized that the system Eq. (12a) and (12b) in the fast time scale becomes

$$\begin{aligned}\frac{d\mathbf{x}_1}{d\tau} &= \varepsilon \mathbf{x}_2, \\ \frac{d\mathbf{x}_2}{d\tau} &= \varepsilon\Big[-\mathbf{H}_{11}\left(\mathbf{x}_1, \varepsilon^2\left(\boldsymbol{\eta}_1 + \bar{\boldsymbol{\xi}}\right)\right)\mathbf{f}_1(\mathbf{x}_1, \mathbf{x}_2) - \mathbf{H}_{12}\left(\mathbf{x}_1, \varepsilon^2\left(\boldsymbol{\eta}_1 + \bar{\boldsymbol{\xi}}\right)\right)\mathbf{f}_2(\mathbf{x}_1, \mathbf{x}_2) \\ &\quad - \mathbf{H}_{11}\left(\mathbf{x}_1, \varepsilon^2\left(\boldsymbol{\eta}_1 + \bar{\boldsymbol{\xi}}\right)\right)\mathbf{g}_1\left(\mathbf{x}_1, \mathbf{x}_2, \varepsilon^2\left(\boldsymbol{\eta}_1 + \bar{\boldsymbol{\xi}}\right), \varepsilon\boldsymbol{\eta}_2\right) \\ &\quad - \mathbf{H}_{12}\left(\mathbf{x}_1, \varepsilon^2\left(\boldsymbol{\eta}_1 + \bar{\boldsymbol{\xi}}\right)\right)\mathbf{g}_2\left(\mathbf{x}_1, \mathbf{x}_2, \varepsilon^2\left(\boldsymbol{\eta}_1 + \bar{\boldsymbol{\xi}}\right), \varepsilon\boldsymbol{\eta}_2\right) \\ &\quad - \mathbf{H}_{12}\left(\mathbf{x}_1, \varepsilon^2\left(\boldsymbol{\eta}_1 + \bar{\boldsymbol{\xi}}\right)\right)\left(\boldsymbol{\eta}_1 + \bar{\boldsymbol{\xi}}\right) + \mathbf{H}_{11}\left(\mathbf{x}_1, \varepsilon^2\left(\boldsymbol{\eta}_1 + \bar{\boldsymbol{\xi}}\right)\right)\mathbf{T}\Big]\end{aligned} \tag{14a}$$

$$\begin{aligned}\frac{d\boldsymbol{\eta}_1}{d\tau} &= \boldsymbol{\eta}_2, \\ \frac{d\boldsymbol{\eta}_2}{d\tau} &= -\mathbf{H}_{21}\left(\mathbf{x}_1, \varepsilon^2\left(\boldsymbol{\eta}_1 + \bar{\boldsymbol{\xi}}\right)\right)\mathbf{f}_1(\mathbf{x}_1, \mathbf{x}_2) - \mathbf{H}_{22}\left(\mathbf{x}_1, \varepsilon^2\left(\boldsymbol{\eta}_1 + \bar{\boldsymbol{\xi}}\right)\right)\mathbf{f}_2(\mathbf{x}_1, \mathbf{x}_2) \\ &\quad - \mathbf{H}_{21}\left(\mathbf{x}_1, \varepsilon^2\left(\boldsymbol{\eta}_1 + \bar{\boldsymbol{\xi}}\right)\right)\mathbf{g}_1\left(\mathbf{x}_1, \mathbf{x}_2, \varepsilon^2\left(\boldsymbol{\eta}_1 + \bar{\boldsymbol{\xi}}\right), \varepsilon\boldsymbol{\eta}_2\right) \\ &\quad - \mathbf{H}_{22}\left(\mathbf{x}_1, \varepsilon^2\left(\boldsymbol{\eta}_1 + \bar{\boldsymbol{\xi}}\right)\right)\mathbf{g}_2\left(\mathbf{x}_1, \mathbf{x}_2, \varepsilon^2\left(\boldsymbol{\eta}_1 + \bar{\boldsymbol{\xi}}\right), \varepsilon\boldsymbol{\eta}_2\right) \\ &\quad - \mathbf{H}_{22}\left(\mathbf{x}_1, \varepsilon^2\left(\boldsymbol{\eta}_1 + \bar{\boldsymbol{\xi}}\right)\right)\left(\boldsymbol{\eta}_1 + \bar{\boldsymbol{\xi}}\right) + \mathbf{H}_{21}\left(\mathbf{x}_1, \varepsilon^2\left(\boldsymbol{\eta}_1 + \bar{\boldsymbol{\xi}}\right)\right)\mathbf{T}\end{aligned} \tag{14b}$$

where the new fast variables $\boldsymbol{\eta}_1$ and $\boldsymbol{\eta}_2$ are defined as

$$\boldsymbol{\eta}_1 = \mathbf{z}_1 - \bar{\boldsymbol{\xi}} = \mathbf{z}_1 - \bar{\mathbf{z}}_1, \ \boldsymbol{\eta}_2 = \mathbf{z}_2 \tag{15}$$

Now setting $\varepsilon = 0$ in Eqs. (14a) and (14b) gives $\frac{d\mathbf{x}_1}{d\tau} = \frac{d\mathbf{x}_2}{d\tau} = 0$; i.e., $\mathbf{x}_1$ and $\mathbf{x}_2$ are constant in the boundary layer. Furthermore, it can be recognized that $\mathbf{g}_1(\mathbf{x}_1, \mathbf{x}_2, 0, 0) = 0$ and $\mathbf{g}_2(\mathbf{x}_1, \mathbf{x}_2, 0, 0) = 0$, since, by definition, those terms are representative of products of the components of $\mathbf{x}_1$ and/or $\mathbf{x}_2$ with the components of $\varepsilon^2\mathbf{z}_1$ and/or $\varepsilon\mathbf{z}_2$. Therefore, the fast subsystem can be found to be

$$\begin{aligned}\frac{d\boldsymbol{\eta}_1}{d\tau} &= \boldsymbol{\eta}_2, \\ \frac{d\boldsymbol{\eta}_2}{d\tau} &= -\mathbf{H}_{22}(\ \bar{\mathbf{x}}_1, 0)\boldsymbol{\eta}_1 + \mathbf{H}_{21}(\bar{\mathbf{x}}_1, 0)\left(\mathbf{T} - \bar{\mathbf{T}}\right)\end{aligned} \tag{16}$$

Which is a linear system parameterized in the slow variables $\bar{x}_1$.

3.2. Composite control

As evidenced by the two subsystems Eq. (13) and Eq. (16), a composite control strategy [14] can be pursued. The design of a feedback control for the full system can be split into two separated designs of feedback controls T and $\mathbf{T}_f$ for the two reduced-order systems; formally

$$\mathbf{T} = \bar{\mathbf{T}}(\bar{\mathbf{x}}_1, \bar{\mathbf{x}}_2) + \mathbf{T}_f(\bar{\mathbf{x}}_1, \boldsymbol{\eta}_1, \boldsymbol{\eta}_2) \tag{17}$$

where $\bar{T}(\bar{x}_1, \bar{x}_2)$ is the slow control, and $\mathbf{T}_f(\bar{x}_1, \boldsymbol{\eta}_1, \boldsymbol{\eta}_2)$ is the fast control.

As far as the slow control is concerned, the computed torque control developed for rigid manipulators as shown previously can be utilized and the slow control is given by

$$\bar{\mathbf{T}} = \mathbf{M}_{11}\left[\ddot{\bar{\boldsymbol{\theta}}}_d + \mathbf{k}_v\left(\dot{\boldsymbol{\theta}}_d - \dot{\bar{\boldsymbol{\theta}}}\right) + \mathbf{k}_p\left(\boldsymbol{\theta}_d - \bar{\boldsymbol{\theta}}\right)\right] + \mathbf{f}_1 \tag{18}$$

where $\mathbf{k}_p$ and $\mathbf{k}_v$ are the position and velocity feedback gain matrices respectively.

At this point, singular perturbation theory requires that the boundary layer system Eq. (16) be uniformly stable along the equilibrium trajectory $\bar{\zeta}$ given by Eq. (9). This can be accomplished if the pair

$$\mathbf{A} = \begin{bmatrix} \mathbf{0} & \mathbf{I} \\ -\mathbf{H}_{22} & \mathbf{0} \end{bmatrix}, \ \mathbf{B} = \begin{bmatrix} \mathbf{0} \\ \mathbf{H}_{21} \end{bmatrix} \tag{19}$$

is uniformly able to be stabilized for any slow trajectory $\bar{\mathrm{x}}_1(t)$. Assuming that this holds, a fast state feedback control of the type

$$\mathbf{T}_f = \mathbf{k}_{pf}(\bar{\mathbf{x}}_1)\boldsymbol{\eta}_1 + \mathbf{k}_{vf}(\bar{\mathbf{x}}_1)\boldsymbol{\eta}_2 \tag{20}$$

will stabilize the boundary layer system Eq. (16) to $\boldsymbol{\eta}_1 = \mathbf{0}$ ($\mathbf{z}_1 = \bar{\zeta}$) and $\boldsymbol{\eta}_2 = \mathbf{0}$ ($\mathbf{z}_2 = \mathbf{0}$). Since the main purpose of flexible manipulator control is to damp out the deflections at steady state as fast as possible, the fast control Eq. (20) can be designed as an optimal control for the boundary layer. To show how fast and slow controller work together, a block diagram for the composite control law is shown in Fig. 1.

Under the above conditions, a fundamental result in singular perturbation theory ensures that the state vectors of the full system can be approximated by

$$\mathbf{x}_1 = \bar{\mathbf{x}}_1 + \mathbf{O}(\varepsilon), \ \mathbf{x}_2 = \bar{\mathbf{x}}_2 + \mathbf{O}(\varepsilon), \tag{21a}$$

$$\mathbf{z}_1 = \bar{\boldsymbol{\zeta}} + \boldsymbol{\eta}_1 + \mathbf{O}(\varepsilon), \ \mathbf{z}_2 = \boldsymbol{\eta}_2 + \mathbf{O}(\varepsilon). \tag{21b}$$

where the operator $\mathbf{O}(\varepsilon)$ means the order of magnitude of ε. Under the slow control Eq. (18), $\boldsymbol{\theta}$ and $\dot{\boldsymbol{\theta}}$ will tend respectively to $\boldsymbol{\theta}_d$ and $\dot{\boldsymbol{\theta}}_d$. The fast control Eq. (20) will derive $\boldsymbol{\eta}_1$ and $\boldsymbol{\eta}_2$ to zero. The goal of following a reference model for the joint variables and stabilizing the deflections around the equilibrium trajectory, naturally set up by the rigid system under the slow control, is then achieved by an $\mathbf{O}(\varepsilon)$ approximation. This is the typical result of a singular perturbation approach.

4. Numerical example

A one-link flexible arm, moves in the horizontal plane, is used to investigate the effect of the joint inertia on the selection of the controller type. The arm is as shown in Fig. 2. The composite control strategy is compared with the computed torque method. Step input of the manipulator is commanded. A step change from $\theta = 0^\circ$ to $\theta = 90^\circ$ is assigned. Two sets of simulations are presented. In the first set, the joint inertia of the arm is considered. In the second set, the joint inertia of the manipulator is considered to be zero. The performance of the manipulator under the composite control and under the computed torque control, in both cases including and excluding the joint inertia is discussed.

The gains of the computed torque control are obtained based on the smallest natural frequency of the flexible arm which is computed using the following equation [15]

$$\omega_1 = (a_1)^2 \sqrt{\frac{EI}{mL^4}} \tag{22}$$

where a_1 is the first eigenvalue, m is the mass per unit length of the beam, EI is the flexural rigidity of the beam, and L is the beam length.

The beam considered here is made of aluminum alloy with density $\rho = 2500$ kg/m^3 and $E = 82$ GPa, and its cross sectional area $A = 6.67 \times 10^{-5}$ m^2. This leads to $m = 0.167$ kg/m. The length of the beam $L = 1.2$ m, and its flexural rigidity $EI = 60$ N m^2. This

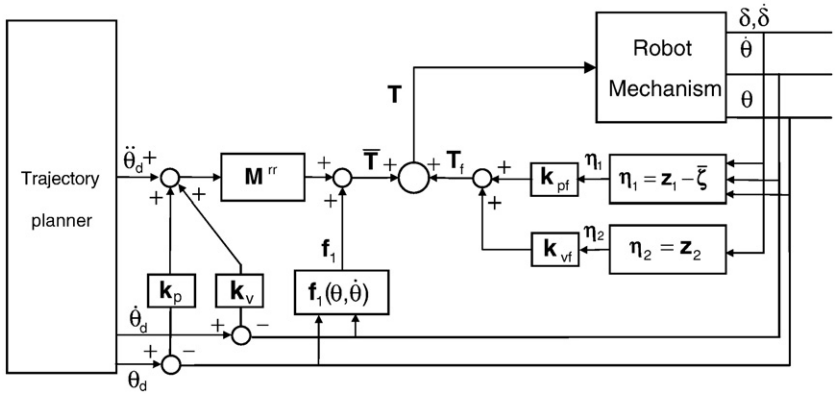

Fig. 1. Composite control block diagram.

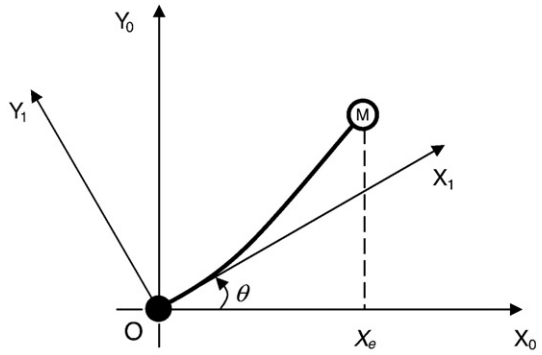

Fig. 2. One-link flexible-arm.

gives the smallest natural frequency of the beam to be approximately equal to 26 rad/s. And to avoid excitation of any of the natural frequencies, the control gains are obtained by setting ω_n in the following equations [13] to be 4 rad/s

$$k_p = \omega_n^2,\ k_v = 2\omega_n \tag{23}$$

The control gains are given as $k_p = 16$ and $k_v = 8$.

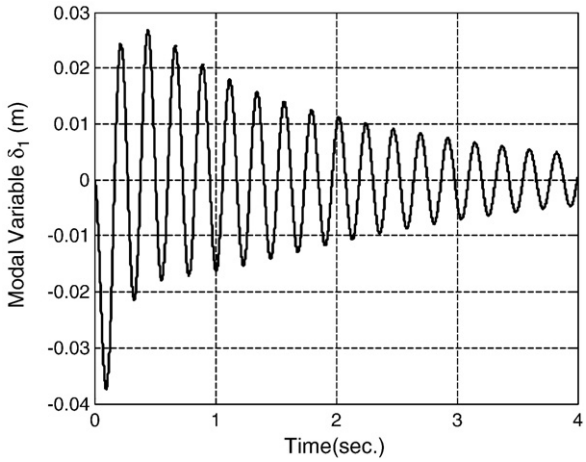

Fig. 3. First modal variable δ_1 (computed torque control) with joint inertia.

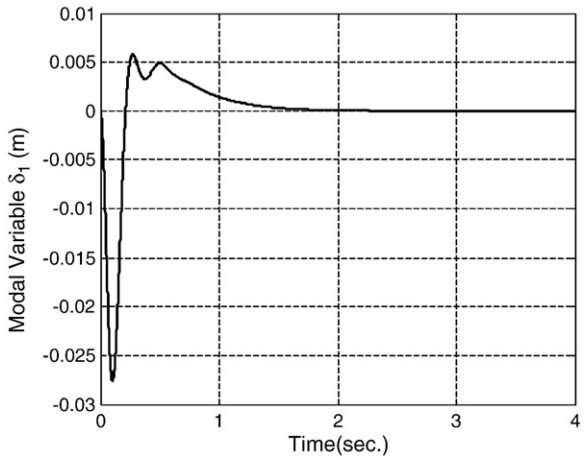

Fig. 4. First modal variable δ_1 (composite control) with joint inertia.

The fast control Eq. (20) can be chosen according to the well-known Linear Quadratic Regulator **LQR** technique [16]. The weighing matrices of the regulator **Q** and **R** are chosen as $\mathbf{Q} = 30\mathbf{I}$ and $\mathbf{R} = 5\mathbf{I}$, where the Larger **Q** is the more emphasis the optimal control places on returning the system to zero. And increasing **R** has the effect of reducing the amount of the control effort allowed,

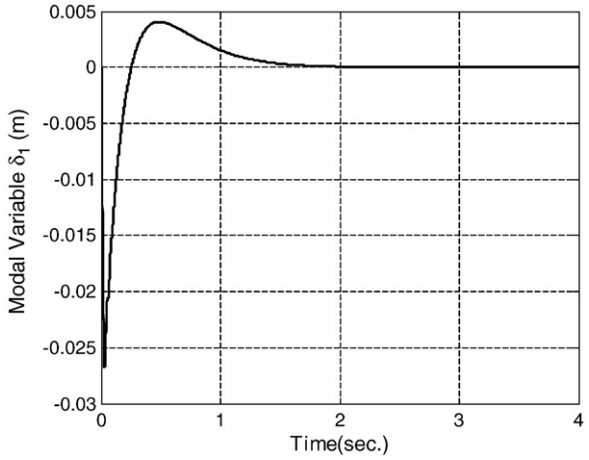

Fig. 5. First modal variable δ_1 (computed torque control) without joint inertia.

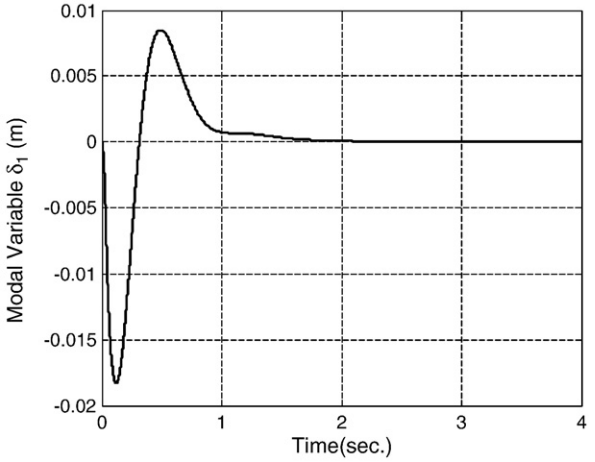

Fig. 6. First modal variable δ_1 (Composite control) without joint inertia.

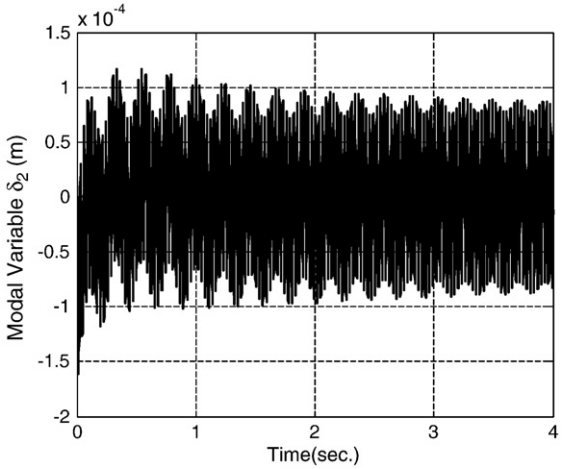

Fig. 7. Second modal variable δ_2 (computed torque control) with joint inertia.

and hence actuator saturation can be avoided. As far as the joint inertia is considered, the gain matrices of the fast sub-system k_{pf} and k_{vf} are respectively [−0.1772 −2.8513] and [−2.9389 −2.4436]. And as the system of zero joint inertia is considered, the gain matrices of the fast sub-system k_{pf} and k_{vf} are respectively [−0.4380−17.6052] and [−2.9425 −2.0143].

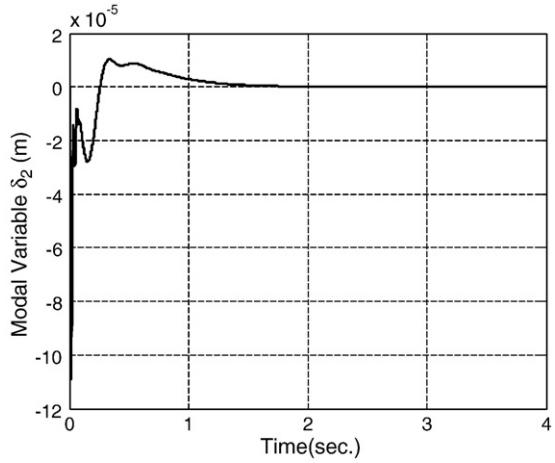

Fig. 8. Second modal variable δ_2 (composite control) with joint inertia.

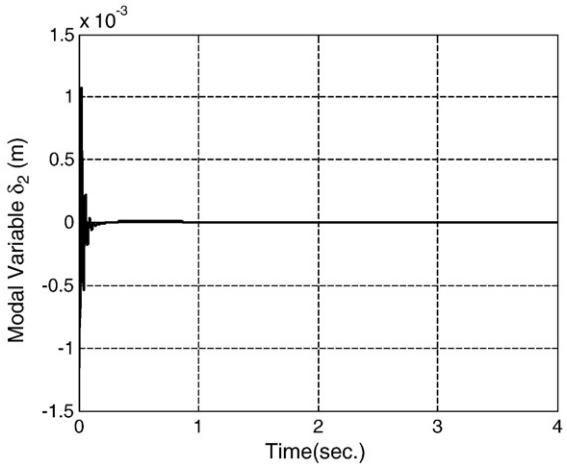

Fig. 9. Second modal variable δ_2 (computed torque control) without joint inertia.

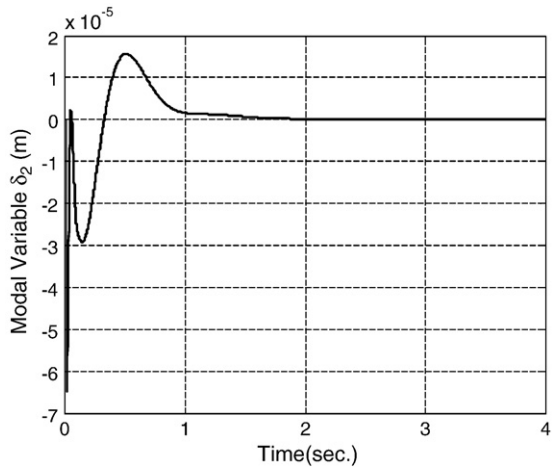

Fig. 10. Second modal variable δ_2 (composite control) without joint inertia.

The performance of the two controllers on both systems (with and without joint inertia) is shown in the following figures. The first modal variable δ_1 of the arm under the computed torque control and the composite control, where the joint inertia is included, are shown in Figs. 3 and 4, respectively. As the joint inertia is not included, the first modal variable δ_1 of the arm under the computed torque control and the composite control, are shown in Figs. 5 and 6, respectively.

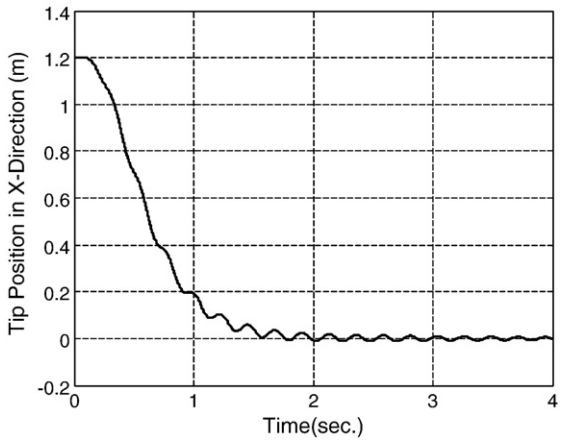

Fig. 11. Tip position along X_0 (computed torque control) with joint inertia.

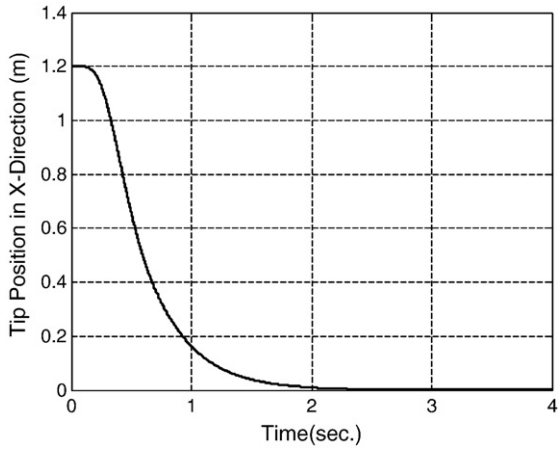

Fig. 12. Tip position along X_0 (composite control) with joint inertia.

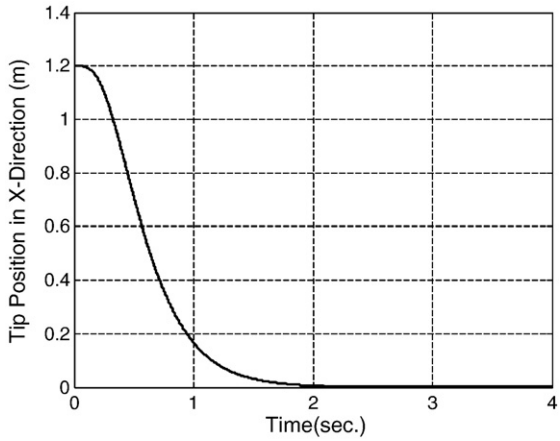

Fig. 13. Tip position along X_0 (computed torque control) without joint inertia.

The maximum value reached by δ_1, under the computed torque control, as the joint inertia is considered is -0.038 m, where the oscillation of the arm extends beyond 4 sec. Under the composite control, and consideration of the joint inertia, the maximum value reached by δ_1 is -0.027 m, and the oscillation of the arm disappears after 1.8 s. Figs. 4 and 5 show that the

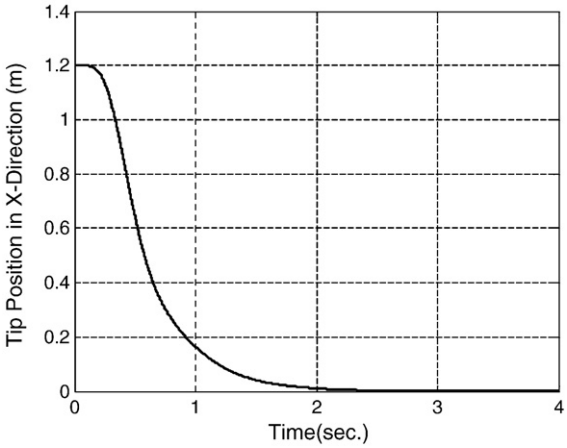

Fig. 14. Tip position along X_0 (composite control) without joint inertia.

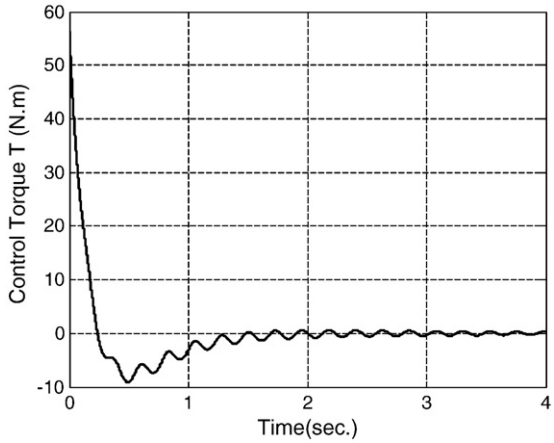

Fig. 15. Control torque T (computed torque control) with joint inertia.

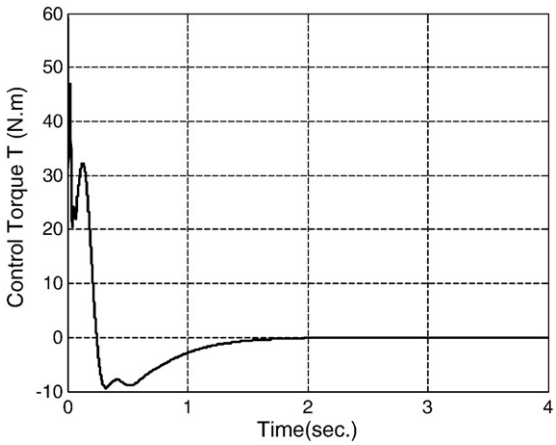

Fig. 16. Control torque T (composite control) with joint inertia.

maximum value of δ_1 is -0.027 m, under the computed torque control, while under the composite control δ_1 reaches a maximum value of -0.018 m. The oscillation of the arm disappears after 1.8 s under both control techniques and neglecting the joint inertia.

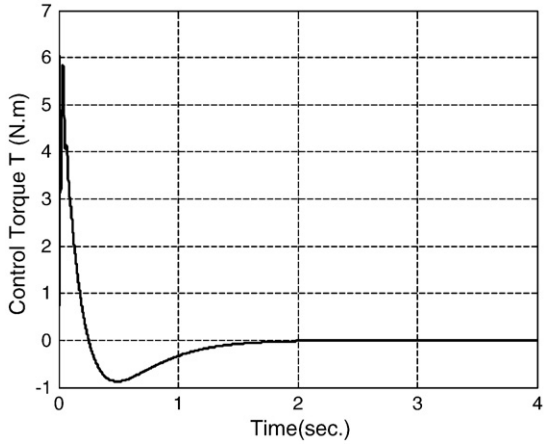

Fig. 17. Control torque T (computed torque control) without joint inertia.

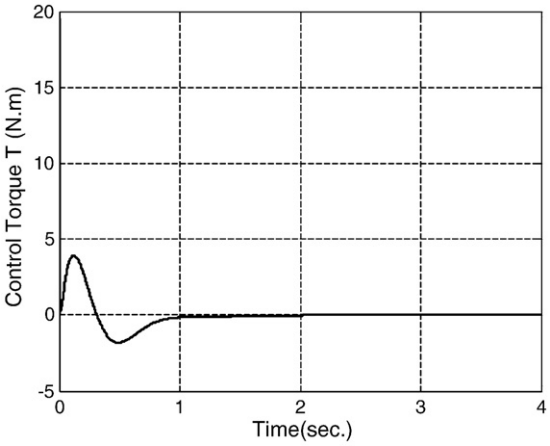

Fig. 18. Control torque T (composite control) with joint inertia.

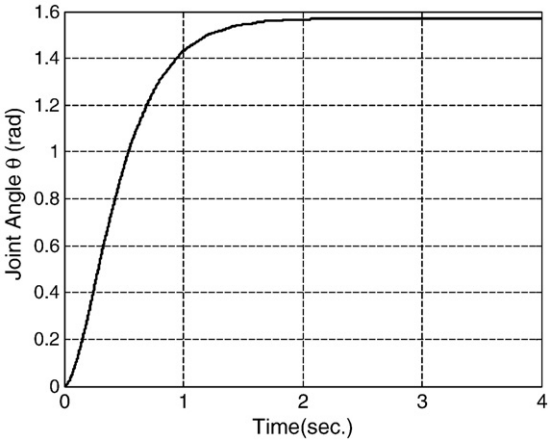

Fig. 19. Joint angle (computed torque control) with joint inertia.

The second modal variable δ_2 of the arm under the computed torque control and the composite control, where the joint inertia is included, are shown in Figs. 7 and 8, respectively. As the joint inertia is not included, the second modal variable δ_2 of the arm under the computed torque control and the composite control are shown in Figs. 9 and 10 respectively.

The maximum value reached by δ_2, under the computed torque control, as the joint inertia is considered is -1.4×10^{-4} m, where the oscillation of the arm extends after 4 s. Under the composite control, and consideration of the joint inertia, the maximum value reached by δ_2 is -11×10^{-5} m, and the oscillation of the arm disappears after 1.8 s. The joint inertia is not considered now. The maximum value of δ_2 is -1.1×10^{-3} m, under the computed torque control. Under the composite control δ_2 reaches a maximum value of -6.5×10^{-5} m. The oscillation of the arm disappears after 1.8 s under both control techniques and neglecting the joint inertia.

As the joint inertia is considered, Figs. 11 and 12 show the tip position along X_0 under the computed torque control and the composite control, respectively. Figs. 13 and 14 show the tip position along X_0 under the computed torque control and the composite control, where the joint inertia is not considered, respectively.

As the joint inertia is considered, and using computed torque control, the arm tip oscillates about the desired position, while using the composite control, the tip position reaches the desired value without oscillations. On the other hand, when the joint inertia is not included, the arm tip reaches the desired position without oscillations under both control strategies.

Figs. 15 and 16 show the control torque under the two control techniques used with consideration of the joint inertia. The control torques used for both control techniques, as the joint inertia is neglected are show in Figs. 17 and 18. These figures show that the total required torque increased as joint inertia is included. This is expected as the total inertia of the overall system increased.

Figs. 19 and 20 show the joint angle step response, when the joint inertia is considered. Figs. 21 and 22 show the joint angle step response, when the joint inertia is considered.

As the joint inertia is considered, the (10% to 90%) rise time in the case of the computed torque control is equal to 0.835 s and in

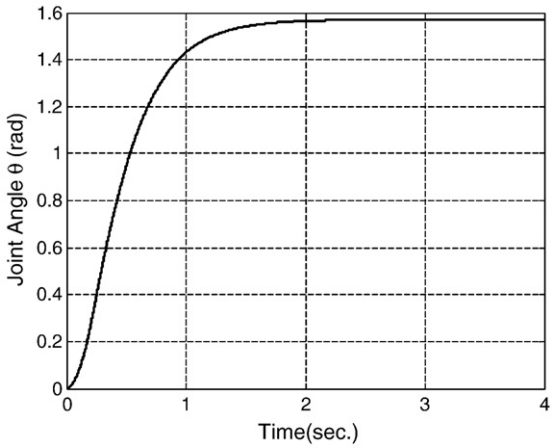

Fig. 20. Joint angle (composite control) with joint inertia.

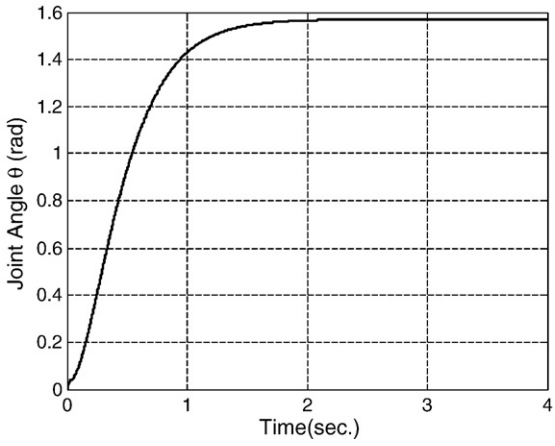

Fig. 21. Joint angle (computed torque control) without joint inertia.

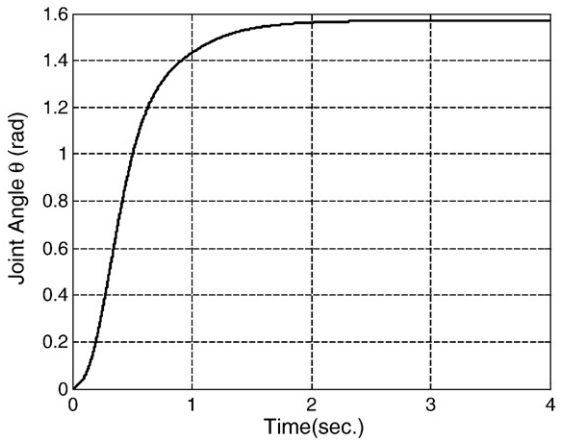

Fig. 22. Joint angle (composite control) without joint inertia.

the case composite control equals 0.803 s. When the joint inertia is neglected, the (10% to 90%) rise time in the case of the computed torque control is equal to 0.834 s and in the case composite control equals 0.775 s.

5. Conclusion

The response of a one-link flexible arm while considering the effect of joint inertia has been investigated. Based on the results, computed torque law would perform equally well with composite control for flexible manipulators as long as the joint inertias are negligible. On the other hand, the introduction of singular perturbation theory, to control flexible manipulator motion, enhanced the system performance, over just computed torque method, in the presence of considerable joint inertias. Also, as long as the joint inertias are negligible, it is preferable to just use computed torque law to control the motion of the flexible arm as its implementation would be easier than that of the composite control.

Appendix A

The fixed-free deflection modes are [15];

$$\phi_j(x) = \left(sin\frac{a_j x}{L} - sinh\frac{a_j x}{L}\right) - \frac{\left(sin\ a_j + sinh\ a_j\right)}{\left(cosa_j + cosh\ a_j\right)}\left(cos\frac{a_j x}{L} - cosh\frac{a_j x}{L}\right),\ \text{for} j = 1, 2. \tag{A.1}$$

For 0.5 payload to link mass ratio, we have $a_1 = 1.42$ and $a_2 = 4.11$.
The equations of motions of a one link flexible arm can be written in the following form,

$$\begin{bmatrix} M_{11} & M_{12} & M_{13} \\ M_{21} & M_{22} & M_{23} \\ M_{31} & M_{32} & M_{33} \end{bmatrix} \begin{bmatrix} \ddot{\theta} \\ \ddot{\delta}_1 \\ \ddot{\delta}_2 \end{bmatrix} + \begin{bmatrix} f_1 \\ f_{21} \\ f_{22} \end{bmatrix} + \begin{bmatrix} g_1 \\ g_{21} \\ g_{22} \end{bmatrix} + \begin{bmatrix} 0 \\ K\begin{bmatrix} \delta_1 \\ \delta_2 \end{bmatrix} \end{bmatrix} = \begin{bmatrix} T_1 \\ 0 \\ 0 \end{bmatrix} \tag{A.2}$$

Where the elements of the previous equation are given as:

$$M_{11} = J_h + J_p + \frac{1}{3}mL^2 + M_pL^2 \tag{A.3}$$

$$M_{12} = 2.33741\frac{J_p}{L^2} + 0.444843\ m + 1.6002\ M_p \tag{A.4}$$

$$M_{13} = -6.89773\frac{J_p}{L^2} + 0.381995\ m - 0.525115\ M_p \tag{A.5}$$

$$M_{21} = M_{12} \tag{A.6}$$

$$M_{22} = 5.46349\frac{J_p}{L^2} + 0.615m + 2.56M_p \tag{A.7}$$

$$M_{23} = -16.1228\frac{J_p}{L^2} + 0.4236m - 0.8403M_p \tag{A.8}$$

$$M_{31} = M_{13} \tag{A.9}$$

$$M_{32} = M_{23} \tag{A.10}$$

$$M_{33} = 47.5786\frac{J_p}{L^2} + 0.87754\, m + 0.275745\, M_p \tag{A.11}$$

$$\begin{bmatrix} f_1 \\ f_{21} \\ f_{22} \end{bmatrix} = \begin{bmatrix} 0 \\ 0 \\ 0 \end{bmatrix} \tag{A.12}$$

$$g_1 = 0 \tag{A.13}$$

$$g_{21} = -0.615m\delta_1\dot{\theta}^2 - 2.5072M_p\delta_1\dot{\theta}^2 - 0.42357m\delta_2\dot{\theta}^2 + 0.8403M_p\delta_2\dot{\theta}^2 \tag{A.14}$$

$$g_{22} = -0.4236m\delta_1\dot{\theta}^2 + 0.8403M_p\delta_1\dot{\theta}^2 - 0.8775m\delta_2\dot{\theta}^2 - 0.2757M_p\delta_2\dot{\theta}^2 \tag{A.15}$$

$$\mathbf{K} = \begin{bmatrix} 7.7055\dfrac{EI}{L^3} & 0 \\ 0 & 290.059\dfrac{EI}{L^3} \end{bmatrix} \tag{A.16}$$

where

beam mass $m = 0.2$ kg, payload mass $M_p = 0.1$ kg, payload inertia $J_p = 0.001$ kg.m^2
joint inertia $J_h = 2$ kg m^2, beam length $L = 1.2$ m, flexural rigidity $EI = 60$ N m^2

References

[1] Z. Mohamed, J.M. Martins, M.O. Tokhi, J. da Costa, M. Botto, Vibration control of a very flexible manipulator system, Control Engineering Practice 13 (2005) 267–277.
[2] B. Subudhi, A.S. Morris, On the singular perturbation approach to trajectory control of a multilink manipulator with flexible links and joints, Proceedings of the Institution of Mechanical Engineers, Journal of Systems & Control Engineering 215 (6) (2001) 587–598.
[3] A. De Luca, Trajectory Control of Flexible Manipulators, Lecture notes in Control and Information Sciences, Vol. 230, Springer, Berlin, 1998, pp. 83–104.
[4] R.J. Theodore, A. Ghosal, Robust control of multilink flexible manipulators, Mechanism and Machine Theory 38 (2003) 367–377.
[5] S. Ider, M. Ozgoren, V. Ay, Trajectory tracking control of robots with flexible links, Mechanism and Machine Theory 37 (2002) 1377–1394.
[6] Y. Aoustin, A Formal'sky, on the feedforward torques and reference trajectory for flexible two-link arm, Multibody System Dynamics 3 (1999) 241–265.
[7] A.H. Nayfeh, Introduction to Perturbation Techniques, Wiley, 1993.
[8] B. Siciliano, W.J. Book, A singular perturbation approach to control of lightweight flexible manipulators, The International Journal of Robotics Research 7 (4) (1988) 79–90.
[9] Sang-Ho Lee, Chong-Won Lee, Hybrid control scheme for robust tracking of two-link flexible manipulator, Journal of Intelligent and Robotic Systems 34 (2002) 431–452.
[10] A. Sanz, V. Exebarria, Experimental control of a two-D of flexible robot manipulator by optimal and sliding methods, Journal of Intelligent and Robotic Systems 46 (2006) 95–110.
[11] W.J. Book, Recursive Lagrangian dynamics of flexible manipulator arms via transformation matrices, The International Journal of Robotics Research 3 (3) (1984) 87–101.
[12] De Luca, B. Siciliano, Closed-form dynamic model of planar multilink lightweight robots, Systems, Man and Cybernetics, IEEE Transactions 21 (4) (1991) 826–839.
[13] M. Spong, S. Hutchinson, M. Vidyasagar, Robot Modeling and Control, Wiley, 2006.
[14] PetarV. Kokotovic, Applications of singular perturbation techniques to control problems, Society for Industrial and Applied Mathematics 26 (4) (1984) 501–550.
[15] L. Meirovitch, Fundamentals of Vibrations, McGraw Hill, 2001.
[16] K. Ogata, Modern Control Engineering, Prentice-Hall, 2002.